DOI: https://doi.org/10.54393/fbt.v4i01.63

FUTURISTIC BIOTECHNOLOGY

https://fbtjournal.com/index.php/fbt
ISSN (E): 2959-0981, (P): 2959-0973
Volume 4, Issue 1 (Jan-Mar 2024)

Original Article

Syzygium cumini-mediated Green Synthesis of Magnesium Oxide Nanoparticles and Evaluation of their Antibacterial, Antileishmanial, and Antioxidant Activities

Suliman Syed[1], Arshad Islam[2*], Ajmal Khan[1], Iftikhar Ahmad[1], Tahir Salam[1] and Nadia Irfan[3]

[1]Institute of Biotechnology and Microbiology, Bacha Khan University, Charsadda, Pakistan
[2]Department of Pathology, Government Lady Reading Hospital Medical Teaching Institution, Peshawar, Pakistan
[3]Department of Biotechnology, Abdul Wali Khan University, Mardan, Pakistan

ARTICLE INFO

Keywords:
Magnesium Oxide Nanoparticles, *Syzygium cumini*, Antibacterial, Antileishmanial, Antioxidant

How to Cite:
Syed, S., Islam, A., Khan, A., Ahmad, I., Salam, T., & Irfan, N. (2024). *Syzygium cumini*-mediated Green Synthesis of Magnesium Oxide Nanoparticles and Evaluation of their Antibacterial, Antileishmanial, and Antioxidant Activities : *Syzygium cumini-mediated* Green Synthesis of Magnesium Oxide Nanoparticles . *Futuristic Biotechnology,* 4(01). https://doi.org/10.54393/fbt.v4i01.63

***Corresponding Author:**
Arshad Islam
Department of Pathology, Government Lady Reading Hospital Medical Teaching Institution, Peshawar, Pakistan
arshad.cgl@gmail.com

Received Date: 18th October, 2023
Acceptance Date: 4th March, 2024
Published Date: 31st March, 2024

ABSTRACT

Green protocols for the synthesis of nanoparticles have gained significant attention due to their environmental friendliness, ease, and cost-effectiveness. **Objectives:** to synthesize magnesium oxide nanoparticles (MgO-NPs) using aqueous leaves extract of *Syzygium cumini* plant, and to investigate the antimicrobial and antioxidant potential of the synthesized NPs. **Methods:** The synthesis of MgO-NPs was achieved by mixing a solution of magnesium nitrate ($Mg(NO_3)_2$ with an aqueous extract obtained from *S. cumini* leaves to reduce the Mg^+ ions. These NPs were characterized by X-ray diffraction (XRD), Fourier-Transform Infrared (FTIR) Spectroscopy analysis, Scanning electron microscopy (SEM), and Energy-dispersive X-ray (EDX) analysis. **Results:** The transformation in color of the solution from yellow to deep brown along with the UV absorption peak at 294 nm showed the effective synthesis of MgO-NPs. SEM and XRD data revealed cubic-shaped NPs with an average size of 23.73 nm. EDX analysis confirmed the presence of magnesium and oxygen in the sample at 31.85% and 35.11% weight percentages, respectively. The antibacterial evaluation demonstrated effectiveness against the gram-negative strains *Citrobacter koseri* and *Pseudomonas aeruginosa*, with inhibition zones of 28.1 ± 1.25 mm and 27.8 ± 1.25 mm, respectively. MgO-NPs also showed *antileishmanial* potential against *Leishmania tropica* promastigotes (68.41 ± 0.05% inhibition at 1000µg/ml). Furthermore, the NPs exhibited antioxidant properties (75.12 ± 4.29% at 1 mg/ml) as determined by the DPPH radical scavenging assay. **Conclusions:** MgO-NPs synthesized using *S. cumini* plant leaves extract hold promises as agents for antibacterial, antileishmanial, and antioxidant applications.

INTRODUCTION

Nanotechnology involves manipulating materials at the atomic or molecular level, with one dimension in nanometers. Metal nanoparticles (NPs) have recently gained significant attention due to their unique features associated with bulk metals. The distinct characteristics of nanoparticles at the nanoscale directly impact their various physical and chemical properties [1, 2]. Due to their unique properties, nanoparticles have the potential to be used as a new antimicrobial drug to combat the growing threat of infectious diseases and antibiotic resistance [3]. Various techniques are available to synthesize MgO-NPs, including sol-gel synthesis, hydrothermal reflux, chemical gas-phase deposition, and wet precipitation, despite some limitations [4, 5, 6, 7]. Advancements in synthesis have made it possible to create eco-friendly and medically useful substances. These substances have properties in various applications [8]. Synthesis strategies that employ natural extracts and water are known as green synthesis [9]. This method of synthesis is gaining popularity due to its eco-friendliness, simplicity, and non-toxic, especially when using plant extracts. *Syzygium cumini* (Jamblang, Jamun) is a Myrtaceae tree that has spread naturally from its native Asia to South America, Africa, and parts of the US .The *S. cumini* plant has potential in various applications

DOI: https://doi.org/10.54393/fbt.v4i01.63

due to its antimicrobial, anti-inflammatory, and antioxidant properties [11, 12, 13].

Due to its medicinal importance, the plant leaf extract was used as a reducing source for the first time to the synthesized MgO NPs. The nanoparticles were analyzed using UV-vis spectroscopy, Fourier-transform infrared (FTIR) spectroscopy, scanning electron microscopy (SEM), energy-dispersive X-ray (EDX) analysis, and X-ray diffraction (XRD). Furthermore, the NPs were assessed for their antibacterial, antileishmanial, and antioxidant properties.

METHODS

Plant Material and Chemicals

Fresh *Syzygium cumini* leaves were harvested from different areas of district Charsadda, Khyber Pakhtunkhwa, Pakistan, and identified using the flora of Pakistan and verified using the online resource (www.theplantlist.org). Antibiotic discs, magnesium nitrate hexahydrate (Mg $(NO_3)_2 6H_2O$; 98%), nutrient agar (NA), antibiotics (Penicillin, Ciprofloxacin® and Streptomycin), RPMI-1640 culture media, Miltefosine, fetal bovine serum (FBS), ascorbic acid ($C_6H_8O_6$; 99%), DPPH (1,1 Diphenyl-2-picryl hydrazyl), and methanol (CH_3OH; 99.8%) were purchased from Sigma Aldrich® (MA., USA). All chemicals and reagents used in the experiments were of minimum analytical grade and used without modification.

Preparation of *Syzygium cumini* Aqueous Leaf Extract

S. cumini leaves were cleaned with tap water and deionized water to remove dirt and particles. The leaves were dried in the shade and crushed into a fine powder using an electric blender (Daigger Scientific®, USA). 25 g of powder and 250 ml of deionized water were mixed in a water bath for 10 minutes. Then the mixture was incubated in the dark under continuous stirring at 24 ℃, for 12 days. The solution was filtered through Whatman No.1 filter paper, and next, the crude aqueous extract was subjected to water evaporation using a rotary evaporator (RE 100-Pro, Biobase®, China) at 70 ℃. The crude extract was acquired and then placed in an airtight container, where it was stored at a temperature of 5 °C for future utilization.

Green synthesis of MgO NPs

Magnesium oxide nanoparticles were synthesized according to the previously reported protocol with minor modifications. 50 ml (10 mg/mL) of *S. cumini* aqueous leaves extract was dropped into 50 ml (0.1 M) magnesium nitrate aqueous solution at 50 ℃ for 3 hours on a magnetic hotplate stirrer (MS300HS, Korea). After obtaining a solid-liquid dispersion, the mixture was centrifuged at 10,000 rpm for 10 minutes. The excess Mg $(NO_3)_2.6H_2O$ and remaining organic molecules were then removed by washing the residue with de-ionized water. To obtain MgO NPs, the residue was dried for 2 h at 70 °C and then calcined for the same time at 300 °C.

Characterization of the Synthesized NPs

The physical and chemical characteristics of MgO NPs were studied using a variety of characterization techniques. For this purpose, UV-vis spectrophotometer (UV-1800 Spectrophotometer, Shimadzu, Japan) in the range of 200-800 was used to confirm the production of NPs, Fourier transformed infrared spectroscopy (FTIR) (L1600300 Spectrum TWO Lita, UK.) was employed within the range of 4000-400 cm^{-1} to identify the capping and stabilizing molecules. Morphological properties of the NPs were evaluated by scanning electron microscopy (SEM) (JSM 5910, JEOL, Japan), and their elemental structure was determined using EDX (INCA 200, Oxford Instruments, UK.). The thermally annealed samples were analyzed with an X-ray diffractometer (JDX.3532, JEOL, Japan) and the corresponding size was determined using the Scherrer equation [15].

Biological Activities

Antibacterial Activity

The study tested the antibacterial properties of Magnesium Oxide (MgO) nanoparticles using an agar well diffusion assay [16]. The nanoparticles were tested against Gram-negative bacterial strains (*Pseudomonas aeruginosa, Providencia stuartii, Proteus vulgaris, Klebsiella pneumoniae, Citrobacter koseri)* and Gram-positive *(Staphylococcus aureus).* Different concentrations of MgO NPs (25, 50, 75, and 100 µg /mL) were tested for their dose-dependent activity. The test was conducted in triplicate and the average was taken to determine the antibacterial activity.

Anti-leishmanial Activity

Following the approach, the anti-leishmanial efficacy of MgO nanoparticles was investigated [17]. In 96-well microtiter plates supplemented with 10% FBS, 1% (Pen Strep) antibiotic, and 1% HEPES buffer, promastigotes *Leishmania tropica* was grown and then subjected to various doses of nanoparticles over a period of 48-72 hours at a temperature of 25 °C. Following incubation, the viability of promastigotes was determined using a tetrazolium-dye (MTT) colorimetric approach. Percent inhibitions were derived using the following formula:

$$= \left[1 - \left\{\frac{Absorbance of sample}{Absorbance of Control}\right\}\right] \times 100$$

Antioxidant Activity

To evaluate the antioxidant capabilities of NPs and ascorbic acid, the DPPH test was utilized [18]. A mixture of a 1-millimolar DPPH solution and a 50% methanol solution was prepared, and diverse amounts of NPs and ascorbic acid were introduced. The resulting mixture was incubated for 30 minutes, and the absorbance at 517 nm was subsequently measured. The effectiveness of each

DOI: https://doi.org/10.54393/fbt.v4i01.63

compound was evaluated in triplicate, and the scavenging ability was determined using a formula:

$$\text{DPPH scavenging \%} = \frac{A0 - At}{A0} \times 100$$

Where A0 is the control (DPPH) sample absorbance and At is the test sample absorbance.

Statistical Analysis

We analyzed the data using OriginPro® version 9.8, 2021 or GraphPad Prism® version 7.0 and reported the results as the mean ± standard deviation (SD) of triplicates.

RESULTS

Characterization of the Synthesized MgO Nanoparticles

Physical appearance and UV spectroscopy Analysis of MgO-NPs

Figure 1 shows that the aqueous extract of *S. cumini* leaves turned dark brown when magnesium nitrate solution was added. The UV absorption peak (figure 2) was measured at 294 nm, which is specific for MgO-NPs. The band gap energy (4.2eV) and visual evidence suggest that the NPs are small and have a band gap, making them suitable as an antibacterial agent

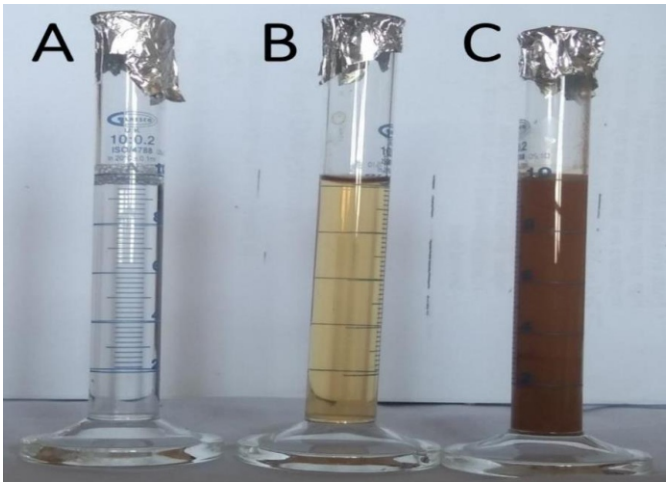

Figure 1: Transformation of yellow color *Syzygium cumini* extract (B) to dark brown (C) upon the addition of colorless magnesium nitrate solution (A).

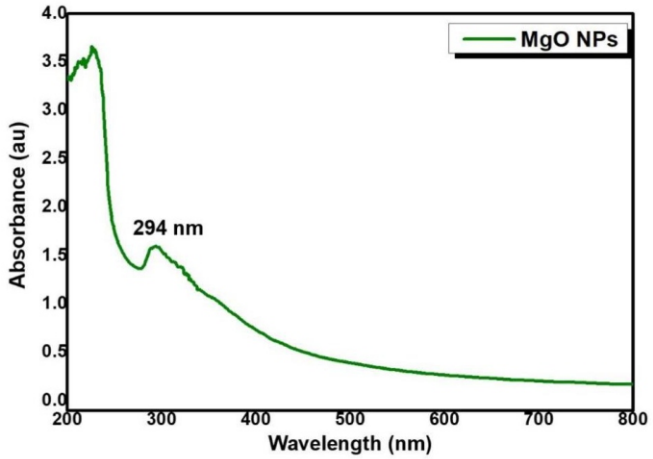

Figure 2: UV-Vis spectra of MgO-NPs using UV-Vis spectrophotometer (UV-1800 Spectrophotometer, Shimadzu, Japan).

Fourier Transform Infrared Spectroscopy (FTIR)

The functional group of MgO-NPs was analyzed by FTIR spectrophotometer in the range 400-4000 cm^{-1} as shown in figure 3. The absorption bands appear at 3690 cm^{-1}, 2217 cm^{-1}, 1784 cm^{-1}, 1352 cm^{-1}, 879 cm^{-1}, 834 cm^{-1}, and 522 cm^{-1}. The two bands at 3690 cm^{-1} and 2217 cm^{-1} were caused by the stretching vibration of the O-H bond. Band 1784 cm^{-1} is attributed to the stretching vibration of C=C, whereas band 1352 cm^{-1} results from the stretching vibration of C=C and the bending of the N-H bond. The bands at 879 cm^{-1} and 834 cm^{-1} correspond to the bending vibration of the C-H and C-O bonds, respectively, whereas the peak at 522 cm^{-1} reveals the presence of MgO.

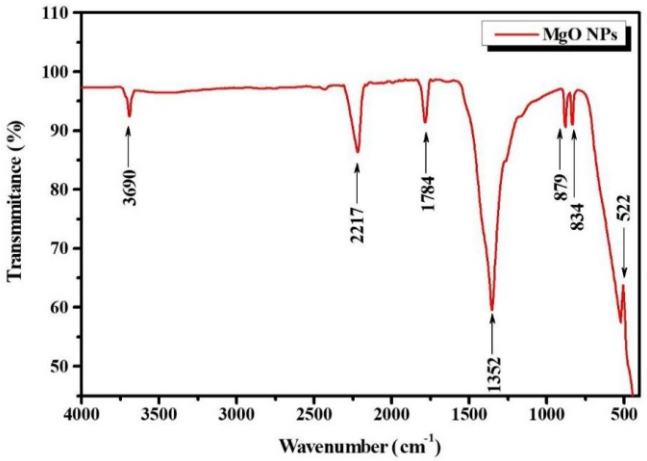

Figure 3: FT-IR spectrums of the synthesized MgO-NPs using (FTIR) (L1600300 Spectrum TWO Lita, UK).

X-Ray Diffraction Analysis (XRD)

The existence of MgO-NPs in the powdered sample was verified using a CuK-X-ray Diffractometer. The peaks shown in Figure. 4 emerged at 2 θ values of 37.82°, 42.58°, 47.82°, and 62.22°, correlating to the lines (111), (200), (220),

DOI: https://doi.org/10.54393/fbt.v4i01.63

and (311), respectively. The diffraction peaks could be readily correlated with specific crystal planes of cubic-phase MgO, and there were no secondary peaks detected. This observation signified the clarity and presence of NPs. The graph's peaks match the literature [19]. The XRD findings show that the NPs are crystalline, and the mean crystallographic size of the resultant MgO-NPs was 23.73 nm. Debye Scherrer's formula was used to calculate the crystalline average size: $D = k\lambda/\beta \cos\theta$ A°. D represents the NPs crystalline size in A°, k the Scherrer constant, λ is the wavelength of X-ray (0.1540 A°), β is the full width at half maximum (FWHM), and θ is the angle of diffraction.

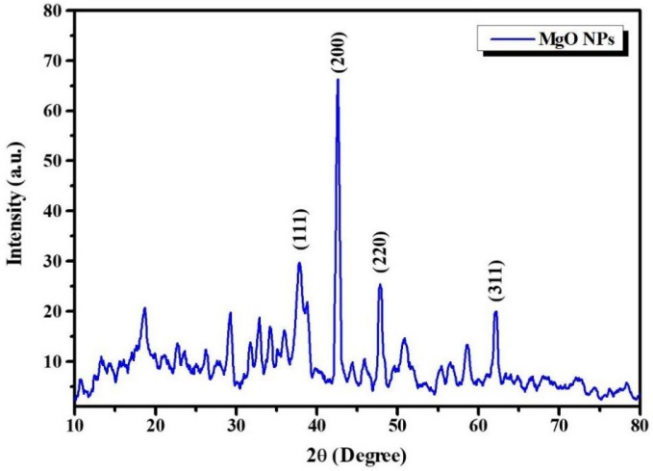

Figure 4: XRD analysis of MgO-NPs using X-ray diffractometer (JDX.3532, JEOL, Japan) in the range of 10-80 degree.

Scanning Electron Microscopy (SEM)

Figure 5 shows the SEM micrographs of MgO-NPs generated under optimal circumstances with a 1-10 µm size scale at different magnifications. The cubic morphology was seen in the marked circles in Figure. 5a of the nanostructures with an average size of 23.73 nm. This observation provided additional support for the XRD analyses' size estimation. Large clusters in Figure. 5b of the SEM micrograph reveals that aggregation was also seen at some locations. However, it is attributable to the selected synthesis approach and the biological abilities of the phytochemicals contained in the plant extract.

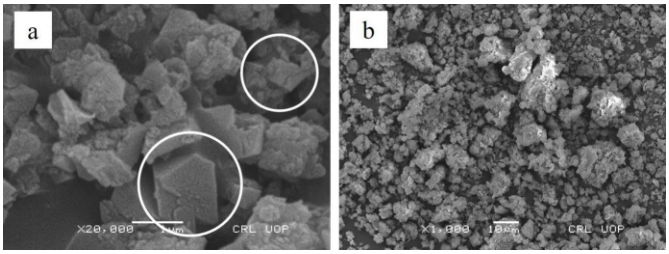

Figure 5: Scanning electron microscope (SEM) images of MgO-NPs, with (a) highlighting cubic morphology as denoted by marked circles, and (b) showcasing NP aggregation leading to large clusters.

Energy-Dispersive X-Ray Analysis

The chemical compositions of the MgO-NPs were determined by EDX analysis. Figure. 6 demonstrates that the NPs are pure, and the presence of Mg and O ions indicates the successful formation via metabolites contained in the aqueous extract of the *S. cumini* plant. The quantitative examination revealed that the samples' weighted percentages of Mg and O ions were 31.85 and 35.11 %, while their atomic percentages were 25.58 and 42.85 %, respectively.

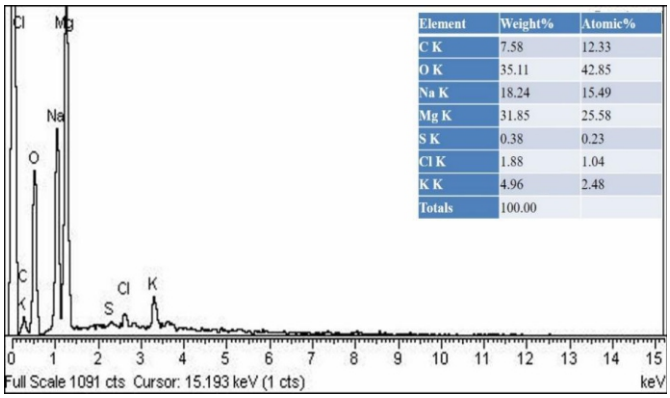

Element	Weight%	Atomic%
C K	7.58	12.33
O K	35.11	42.85
Na K	18.24	15.49
Mg K	31.85	25.58
S K	0.38	0.23
Cl K	1.88	1.04
K K	4.96	2.48
Totals	100.00	

Figure 6: Energy dispersive X-ray spectroscopy of MgO-NPs using EDX (INCA 200, Oxford Instruments, UK).

Biological Applications

Antibacterial Activity

The antibacterial potential of MgO-NPs was investigated by assessing the zone of inhibition against the tested bacterial strains. All bacterial strains were tested with Ciprofloxacin as a positive control as depicted in Figure. 7. Zone of inhibition was 28.1±1.25 mm *(C. koseri),* 27.8 ± 1.25 mm (*P. aeruginosa),* 27.3 ± 1.04 mm *(P. vulgaris),* 25.1 ± 1.04 mm *(P. stuartii),* and 24.8 ± 1.25 mm *(K. pneumoniae)* for gram-negative bacteria and 25.8 ± 0.76 nm for gram-positive bacteria. *C. koseri* (28.1 ± 1.25 mm) was the most susceptible gram-negative strain to the highest concentration. The presence of an inhibitory zone shows that these NPs kill bacteria possibly by disrupting membranes and generating surface oxygen species. Size of inhibitory zone varied by pathogen and NPs concentration (Figure 8). In this work, increasing the concentration (25-100 µg/ml) of MgO-NPs boosted growth inhibition due to nanoparticle diffusion in agar media.

DOI: https://doi.org/10.54393/fbt.v4i01.63

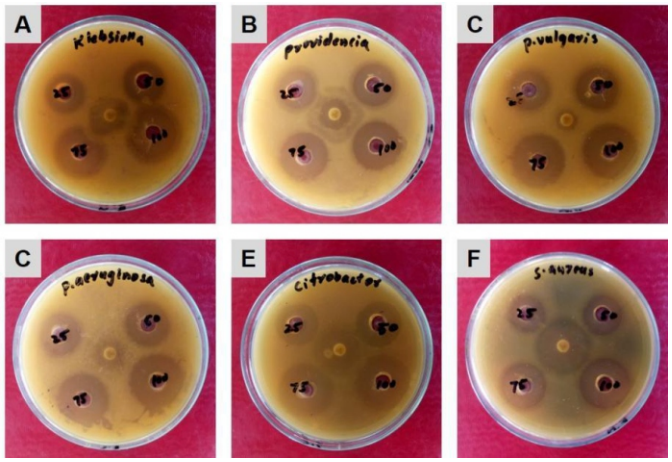

Figure 7: Zones of inhibition induced by MgO-NPs against the assessed bacterial strains. (A) *K. pneumoniae*, (B) *P. stuartii*, (C) *P. vulgaris*, (D) *P. aeruginosa*, (E) C. koseri, and (F) *S. aureus*.

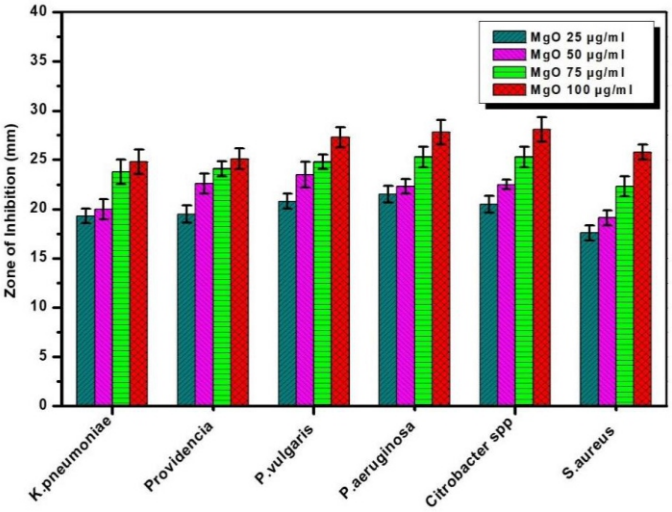

Figure 8: Graphical depiction of the antibacterial potential of MgO-NPs at various concentration (25-100 µg/ml).

Antileishmanial Activity

Our study on the impact of MgO-NPs on the growth of *L. tropica* culture is presented in figure 9. Different concentrations of NPs (250-1000 µg/mL) were used and measured the percentage of inhibition over 48 to 72 hours. To assess the efficacy of the NPs, we compared them to Miltefosine (standard antileishmanial drug) and DMSO, a negative control. Our findings indicated that the inhibition of parasites increased in proportion to the concentration of NPs used. Specifically, at 1000µg/ml, the NPs inhibited 68.41 ± 0.05%, at 500µg/ml they inhibited 55 ± 0.14%, and at 250µg/ml they inhibited 34.03 ± 0.28%. The IC_{50} value was 452µg/ml which suggest that these NPs have the potential to serve as an antileishmanial agent.

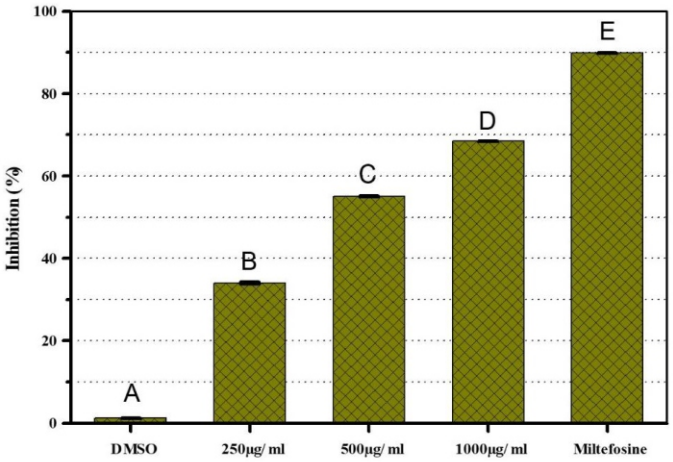

Figure 9: Assessment of Leishmaniasis inhibition by MgO-NPs. (A) represents the inhibition in the negative control using DMSO, while (B, C, D) show the inhibition at different concentrations of MgO-NPs. (E) displays the inhibitory effect of the positive control Miltefosine.

Antioxidant Activity

Absorbance at 517 nm was used to calculate the radical scavenging activity of DPPH. MgO-NPs showed moderate radical scavenging activity and increased effectiveness with concentration (0.1-1 mg/ml). Ascorbic acid (standard antioxidant) exhibited more efficient radical scavenging capability than the NPs (Figure 10). At 1mg/ml, the antioxidant action of the NPs increased from 8.68 ± 0.61% to 75.12 ± 4.29% with an IC50 value of 1.92mg/ml.

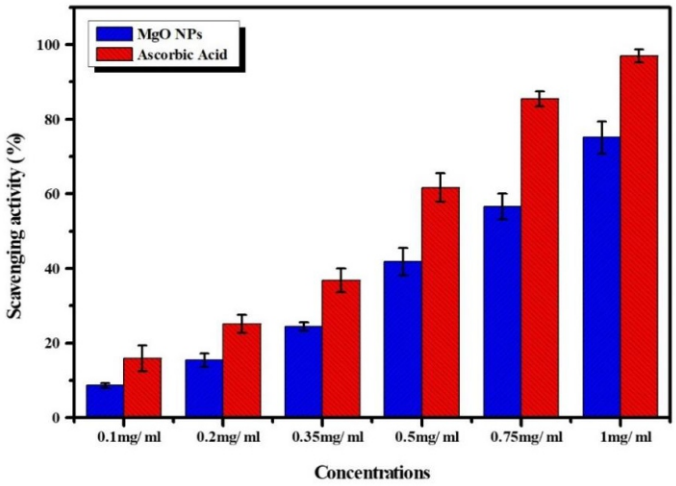

Figure 10: Antioxidant potential of MgO-NPs and ascorbic acid at different concentrations (0.1-1 mg/ml).

DISCUSSION

Color changes and UV-visible spectroscopy analysis indicate the formation of MgO nanoparticles with a sharp peak confirming successful synthesis and predicted band-gap energy [20]. Five absorption bands were observed in the FTIR spectra, showing the presence of hydroxide,

DOI: https://doi.org/10.54393/fbt.v4i01.63

alkynes, amino groups, and magnesium oxide. Reduction in peak intensity confirms the involvement of organic molecules in the synthesis. Peaks in the broader and narrower range indicate the stretching of alkynes and Mg-O vibrations, respectively [21]. The sample has a cubic phase and multiple indexed crystal planes. It's worth noting that no secondary peaks were detected, indicating that the NPs are pure and free from impurities. A published study showed that the synthesized MgO-NPs had a cubic structure and minimal impurities [22]. These NPs under SEM had a cubic morphology with a small size along with clusters which are due to synthetic methods and biological incapacitation of phytochemicals. Elemental analysis confirmed the purity of NPs and suggests the formation through metabolites in the plant. Previously, MgO-NPs were spherical with an average diameter of 36.74 nm, and have aggregated into dense, irregular, pointy flakes [23]. The synthesized substance consistently exhibits antibacterial activity against all strains. NPs may kill bacteria by disrupting the membrane. Increasing the concentration of MgO-NPs enhances their effectiveness. Small size improves their antibacterial properties against both gram-positive and gram-negative bacteria. The increase in surface area results in more active sites on the nanoparticle's surface, displaying significant antibacterial properties [24]. MgO-NPs showed antileishmanial activity against L. tropica promastigotes by increasing concentration led to more inhibition. MgO-NPs also inhibited promastigote infectivity in a dose-dependent manner [25]. Furthermore, our study on the antioxidant potential of NPs found that increasing the concentration of the sample improved their radical scavenging abilities [1].

CONCLUSIONS

The use of *Syzygium cumini* leaf extract is an affordable, eco-friendly, and safe method for producing magnesium oxide nanoparticles (MgO-NPs). The synthesized material underwent comprehensive analysis using various techniques, such as UV-Vis, FTIR, EDX, SEM, and XRD. MgO-NPs demonstrated a remarkable ability to fight against pathogenic microorganisms. Furthermore, the NPs showed potential in inducing parasite cytotoxicity, which could be useful in antileishmanial treatments. The NPs also displayed significant antioxidant properties, making them useful as an antioxidant.

Authors Contribution

Conceptualization: SS, AI, AK
Methodology: SS, IA, TS
Formal analysis: SS, AI, NI
Writing-review and editing: AI

All authors have read and agreed to the published version of the manuscript.

Conflicts of Interest

The authors declare no conflict of interest.

Source of Funding

The authors received no financial support for the research, authorship and/or publication of this article.

REFERENCES

[1] Faisal S, Abdullah, Jan H, Shah SA, Shah S, Rizwan M, *et al.* Bio-catalytic activity of novel Mentha arvensis intervened biocompatible magnesium oxide nanomaterials. Catalysts. 2021 Jun; 11(7): 780. doi: 10.3390/catal11070780.

[2] Luyts K, Napierska D, Nemery B, Hoet PH. How physico-chemical characteristics of nanoparticles cause their toxicity: complex and unresolved interrelations. Environmental science: Processes & Impacts. 2013 Nov; 15(1): 23-38. doi: 10.1039/C2EM30237C.

[3] Al-Awsi GR, Alameri AA, Al-Dhalimy AM, Gabr GA, Kianfar E. Application of nano-antibiotics in the diagnosis and treatment of infectious diseases. Brazilian Journal of Biology. 2023 Jan; 84. doi: 10.1590/1519-6984.264946.

[4] Salman KM, Renuka CG. Modified sol-gel technique for the synthesis of pure MgO and ZnO nanoparticles to study structural and optical properties for optoelectronic applications. Materials Today: Proceedings. 2023 Jun.

[5] Todan L, Predoană L, Petcu G, Preda S, Culiță DC, Băran A, *et al*. Comparative Study of MgO Nanopowders Prepared by Different Chemical Methods. Gels. 2023 Aug; 9(8): 624. doi: 10.3390/gels9080624.

[6] Abbas IK, Adim KA. Synthesis and characterization of magnesium oxide nanoparticles by atmospheric non-thermal plasma jet. Kuwait Journal of Science. 2023 May; 50(3): 223-230. doi: 10.1016/j.kjs.2023.05.008.

[7] Yadav P, Saini R, Bhaduri A. Facile synthesis of MgO nanoparticles for effective degradation of organic dyes. Environmental Science and Pollution Research. 2023 Jun; 30(28): 71439-53. doi: 10.1007/s11356-022-21925-0.

[8] Rotti RB, Sunitha DV, Manjunath R, Roy A, Mayegowda SB, Gnanaprakash AP, *et al.* Green synthesis of MgO nanoparticles and its antibacterial properties. Frontiers in Chemistry. 2023 Mar; 11: 1143614. doi: 10.3389/fchem.2023.1143614.

[9] de Jesus RA, de Assis GC, de Oliveira RJ, Costa JA, da Silva CM, Iqbal HM, *et al*. Metal/metal oxide nanoparticles: A revolution in the biosynthesis and medical applications. Nanostructures & Nano-Objects. 2024 Feb; 37: 101071. doi: 10.1016/j.nanoso.2023.101071.

DOI: https://doi.org/10.54393/fbt.v4i01.63

[10] Mandal SK, Das A, Devkota HP, Das N, *Syzygium cumini* (L.) Skeels. In: Belwal T, Bhatt I, Devkota H. Himalayan Fruits, and Berries: Bioactive Compounds, Uses and Nutraceutical Potential. Cambridge. Academic Press. 2022: 403-18. doi: 10.1016/B978-0-323-85591-4.00001-5.

[11] Kumari N, Kumar M, Chaudhary N, Zhang B, Radha, Chandran D, *et al.* Exploring the Chemical and Biological Potential of Jamun (Syzygium cumini (L.) Skeels) Leaves: A Comprehensive Review. Chemistry & Biodiversity. 2023 Sep; 20(9): e202300479. doi: 10.1002/cbdv.202300479.

[12] Qamar M, Akhtar S, Ismail T, Wahid M, Ali S, Nazir Y, *et al.* Syzygium cumini (L.) Skeels extracts; in vivo anti-nociceptive, anti-inflammatory, acute and subacute toxicity assessment. Journal of Ethnopharmacology. 2022 Apr ;287: 114919. doi: 10.1016/j.jep.2021.114919.

[13] Kumar M, Zhang B, Nishad J, Verma A, Sheri V, Dhumal S, *et al.* Jamun (Syzygium cumini (L.) Skeels) Seed: A Review on Nutritional Profile, Functional food properties, health-promoting applications, and safety aspects. Processes. 2022 Oct; 10(11): 2169. doi: 10.3390/pr10112169.

[14] Ali S, Sudha KG, Thirumalaivasan N, Ahamed M, Pandiaraj S, Rajeswari VD, *et al.* Green Synthesis of Magnesium Oxide Nanoparticles by Using Abrus precatorius Bark Extract and Their Photocatalytic, Antioxidant, Antibacterial, and Cytotoxicity Activities. Bioengineering. 2023 Feb ; 10(3): 302. doi: 10.3390/bioengineering10030302.

[15] Zaman A, Uddin S, Mehboob N, Tirth V, Algahtani A, Abbas M, *et al.* Structural Elucidation, Electronic and Microwave Dielectric Properties of Ca (Sn x Ti1–x) 03,(0≤ x≤ 0.8) Lead-Free Ceramics. ACS omega. 2022 Jan; 7(5): 4667-76. doi: 10.1021/acsomega.1c06918.

[16] Gabriel T, Vestine A, Kim KD, Kwon SJ, Sivanesan I, Chun SC. Antibacterial activity of nanoparticles of garlic (allium sativum) extract against different bacteria such as Streptococcus mutans and poryphormonas gingivalis. Applied Sciences. 2022 Mar; 12(7): 3491. doi: 10.3390/app12073491.

[17] Islam A, Ain Q, Munawar A, Corrêa Junior JD, Khan A, Ahmad F, *et al.* Reactive oxygen species generating photosynthesized ferromagnetic iron oxide nanorods as promising antileishmanial agent. Nanomedicine. 2020 Apr; 15(08): 755-71. doi: 10.2217/nnm-20190095.

[18] Riaz M, Altaf M, Ayaz M, Sherkheli MA, Islam A. Antibacterial and antioxidant potential of biosynthesized silver nanoparticles using aqueous root extract of Angilica glauca. Inorganic and Nano-Metal Chemistry. 2020 Aug; 51(10): 1379-85. doi: 10.1080/24701556.2020.1835977.

[19] Pugazhendhi A, Prabhu R, Muruganantham K, Shanmuganathan R, Natarajan S. Anticancer, antimicrobial and photocatalytic activities of green synthesized magnesium oxide nanoparticles (MgONPs) using aqueous extract of Sargassum wightii. Journal of Photochemistry and Photobiology B: Biology. 2019 Jan; 190: 86-97. doi: 10.1016/j.jphotobiol.2018.11.014.

[20] John Sushma N, Prathyusha D, Swathi G, Madhavi T, Deva Prasad Raju B, Mallikarjuna K, *et al.* Facile approach to synthesize magnesium oxide nanoparticles by using Clitoria ternatea—characterization and in vitro antioxidant studies. Applied Nanoscience. 2016 Mar; 6: 437-44. doi: 10.1007/s13204-015-0455-1.

[21] Vergheese M, Vishal SK. Green synthesis of magnesium oxide nanoparticles using Trigonella foenum-graecum leaf extract and its antibacterial activity. Journal of Pharmacognosy and Phytochemistry. 2018 Apr; 7(3): 1193-200.

[22] Moorthy SK, Ashok CH, Rao KV, Viswanathan C. Synthesis, and characterization of MgO nanoparticles by Neem leaves through green method. Materials Today: Proceedings. 2015 Jan; 2(9): 4360-8. doi: 10.1016/j.matpr.2015.10.027.

[23] Ali R, Shanan ZJ, Saleh GM, Abass Q. Green synthesis and the study of some physical properties of MgO nanoparticles and their antibacterial activity. Iraqi Journal of Science. 2020 Feb; 61(2); 266-76. doi: 10.24996/ijs.2020.61.2.9.

[24] Tang ZX, Lv BF. MgO nanoparticles as antibacterial agent: preparation and activity. Brazilian Journal of Chemical Engineering. 2014; 31(3): 591-601. doi: 10.1590/0104-6632.20140313s00002813.

[25] Jebali A, Hekmatimoghaddam S, Kazemi B, Allaveisie A, Masoudi A, Daliri K, *et al.* Lectin coated MgO nanoparticle: its toxicity, antileishmanial activity, and macrophage activation. Drug and Chemical Toxicology. 2014 Oct; 37(4): 400-9. doi: 10.3109/01480545.2013.870192.